Research Article | DOI: 10.5281/zenodo.14511951
www.jnanosam.com

NANOSAM
Journal of NanoScience in Advanced Materials

Synthesis and Characterization of (3-Aminopropyl) triethoxysilane - Derived Silicon Nanoparticles Reduced with Ascorbic Acid

Gülşah Çelik Gül[1#], Çiğdem Ulu[2] and Seda Beyaz[2]

This study explores the influence of synthesis parameters—reaction temperature, time, (3-Aminopropyl)triethoxysilane (APTES), and ascorbic acid (AA)—on the particle size and optical properties of silicon nanoparticles (SiNPs). A total of 22 experiments were conducted, employing UV-visible (UV-Vis) spectroscopy, photoluminescence (PL) spectroscopy, and transmission electron microscopy (TEM) for thorough characterization, with unique observations of color changes over time using periodic UV-Vis measurements. Initial studies at 40, 50, and 60°C for 30 to 120 minutes revealed that higher temperatures and aging enhanced UV absorbance, especially in the 200–250 nm range. A reaction duration of 60 minutes at 50°C optimized particle formation, with PL measurements indicating strong emission around 520 nm. Further tests showed that increased APTES levels shifted absorption to 350–450 nm, with dual peaks indicating specific silicon transitions. Over time, absorption in this range decreased, attributed to unreacted APTES. TEM images revealed spherical, well-dispersed particles with sizes influenced by APTES and AA levels. Higher AA concentrations improved particle formation, particularly in the 200–325 nm range, acting as a reducing agent. When APTES and AA were balanced, smaller particles (8.508±2.832 nm) formed, surrounded by amine-silica chains. These findings offer insights into tailoring SiNP properties for biotechnology, demonstrating the potential to achieve desired size, optical characteristics, and stability through precise parameter adjustments.

1. Introduction

Silicon (Si) is a group IV element in the periodic table, closely related to carbon. It is abundant in nature, often found as silicates or combined with oxygen to form silicon dioxide (SiO_2). Silicon has a strong affinity for oxygen, forming stable Si=O bonds. The primary structural unit of silicon compounds is silicon-oxygen tetrahedron (SiO_4) [1]. As the second most abundant element on Earth, silicon dominates the semiconductor industry. Silicon-based nanomaterials, particularly fluorescent silicon nanoparticles (Si NPs), hold great promise for various optical applications due to their non-toxic nature and potential for biocompatibility [2]

Si NPs have several advantages over other luminescent nanomaterials, including low cost and abundant availability [3]. Their non-toxic composition makes them especially promising for practical applications. Moreover, Si NPs offer versatile, tunable surface functionalities, allowing them to play a significant role in sensing applications [4]. Due to their unique optical properties, solubility, biocompatibility, and photostability, silicon nanomaterials have attracted interest in fields such as energy, catalysis, optoelectronics, and biology [5-7].

Two main approaches for nanoparticle production are “Top-Down” and “Bottom-Up.” In the Top-Down approach, bulk material is broken down into nanoparticles through mechanical or chemical processes. The Bottom-Up approach, however, involves building nanoparticles from atomic or

[1]Department of Veterinary Medicine, Savaştepe Vocational School, Balikesir University, 10145, Balıkesir, Türkiye, [2]Department of Chemistry, Faculty of Science&Art, Balıkesir University, 10145, Balıkesir, Türkiye

#Corresponding author: gulsahcelik9@gmail.com

Keywords: Silicon nanoparticles; Ascorbic acid; (3-aminopropyl)triethoxysilane.

Received: 23 October 2024 | Accepted: 12 November 2024 | Published online: 25 December 2024

molecular structures through chemical reactions [8].

One common method for Si NP synthesis is the sol-gel process, known for its simplicity and ability to introduce functional groups under mild conditions. Additionally, techniques such as the Stöber method and surface modification have been explored for producing Si NPs with specific properties [9].

In this study, water-soluble Si NPs were synthesized using 3-aminopropyltriethoxysilane (APTES) as a silicon source and L-ascorbic acid (AA) as a reducing agent, following a simple and low-cost process at room temperature [10]. This method is advantageous over techniques like Stöber or sol-gel, as it requires fewer chemicals and operates under milder conditions. APTES is one of the most commonly used organosilanes due to its low cost, and the energy demands are minimal since high temperatures are not required for synthesis, making this approach energy-efficient and scalable [11]. Moreover, this method allows for quick production, enabling large-scale manufacturing within a short time in a single reaction system, thereby saving both time and resources.

2. Results and Discussion

In this study, a total of 22 experiments were conducted to investigate the effects of reaction temperature, reaction time, APTES amount, and ascorbic acid amount on the particle size of silicon nanoparticles. To observe these effects, UV absorption spectra, band gap calculations, reflectance graphs, PL graphs, and TEM images were utilized. Additionally, unlike all previous studies in the related literature, the color changes in the samples over time were monitored by remeasuring the UV spectra.

Reaction temperature and time: In order to investigate the effect of reaction temperature and time on the formation of silicon nanoparticles, first 15 experiments were conducted at temperatures of 40, 50, and 60°C for durations of 30, 60, 90, and 120 minutes. Upon examining the UV spectras (figure 2 and figure 3) of these experiments, it was observed that the samples exhibited strong absorption at wavelengths below 300 nm. Since no absorption was detected beyond 450 nm, the graphs are presented within the wavelength range of 200-450 nm.

In the literature, the characteristic absorbance band of Si NPs is reported to be between 200 and 250 nm [7]. This absorbance band was present in the spectra of all synthesized samples, and in addition, absorbance maxima around 265 nm were observed in the 250-300 nm range. This could be attributed to unreacted organosilanes (APTES molecules) [13,14] or luminescent groups surrounding the Si NPs. The intensity of these absorbance peaks generally decreased as the temperature increased. However, in the sample with a reaction time of 90 minutes, the intensity first increased and then decreased with rising temperature.

In the absorbance spectra, the peaks between 200-250 nm broadened and merged with other absorbance bands as the temperature increased, strengthening the overall absorption. Additionally, absorbance in the 300-400 nm range also increased. These observations suggest that the formation of Si NPs with strong UV absorbance accelerates as the temperature increases. As shown in Figure 3, UV absorption analysis of the samples was repeated approximately three months later. In Figure 3, it was observed that the absorption peaks in the 200-250 nm wavelength range strengthened over time in the spectra of all samples. As the samples aged, the absorbance shifted towards shorter wavelengths, and interactions with UV light increased. To better understand the effect of reaction time on the properties of the synthesized samples, seven different reaction durations were specifically studied for the synthesis at 50°C. Based on the data obtained from this set of experiments, a reaction temperature of 50°C and a duration of 60 minutes were selected for investigating the effects of other factors. The color change in the samples over a period of 3 months is also shown in Figure 4.

Photoluminescence (PL) excitation and emission spectra were obtained at room temperature for the syntheses with reaction times of 30 minutes (SiNP5), 60 minutes (SiNP7), and 80 minutes (SiNP9), using a 349 nm wavelength laser for excitation. The emission spectra obtained using PLe spectroscopy are shown in Figure 5. Additionally, another set of PL excitation and emission spectra was recorded after approximately 3 months, with the corresponding graph presented in Figure 6.

As seen in Figure 5, the fluorescence spectra of the Si NP samples demonstrate fluorescence behavior dependent on excitation. The photoluminescence spectra in the figure indicate that the samples strongly absorb light in the UV region and exhibit a broad band spectrum around 520 nm. Similarly, previous literature has reported that the fluorescence emission for Si NPs occurs at 520 nm [10]. Unlike the syntheses conducted at 60 minutes and 80 minutes, the 30-minute reaction showed a narrow band spectrum around 580 nm. The emission intensity at 520 nm decreased as the reaction time increased. The PL peak positions and absorption peaks suggest good optical properties. The intensity of the samples, in descending order, is 5, 7, and 9. The wavelength varies across the emitting regions.

NANOSAM
Journal of NanoScience in Advanced Materials

Table 1. Experimental design.

Number of sample	Degree (°C)	Time (min)	APTES quantity (mL)	AA molarity (M)	AA guantity (mL)
SiNP1	40	30	1.00	0.1	1.25
SiNP2	40	60	1.00	0.1	1.25
SiNP3	40	90	1.00	0.1	1.25
SiNP4	40	120	1.00	0.1	1.25
SiNP5	50	30	1.00	0.1	1.25
SiNP6	50	40	1.00	0.1	1.25
SiNP7	50	60	1.00	0.1	1.25
SiNP8	50	70	1.00	0.1	1.25
SiNP9	50	80	1.00	0.1	1.25
SiNP10	50	90	1.00	0.1	1.25
SiNP11	50	120	1.00	0.1	1.25
SiNP12	60	30	1.00	0.1	1.25
SiNP13	60	60	1.00	0.1	1.25
SiNP14	60	90	1.00	0.1	1.25
SiNP15	60	120	1.00	0.1	1.25
SiNP16	50	60	1.50	0.1	1.25
SiNP17	50	60	2.00	0.1	1.25
SiNP18	50	60	2.50	0.1	1.25
SiNP19	50	60	3.00	0.1	1.25
SiNP20	50	60	1.50	0.1	1.50
SiNP21	50	60	1.50	0.1	2.00
SiNP22	50	60	1.50	0.1	2.50

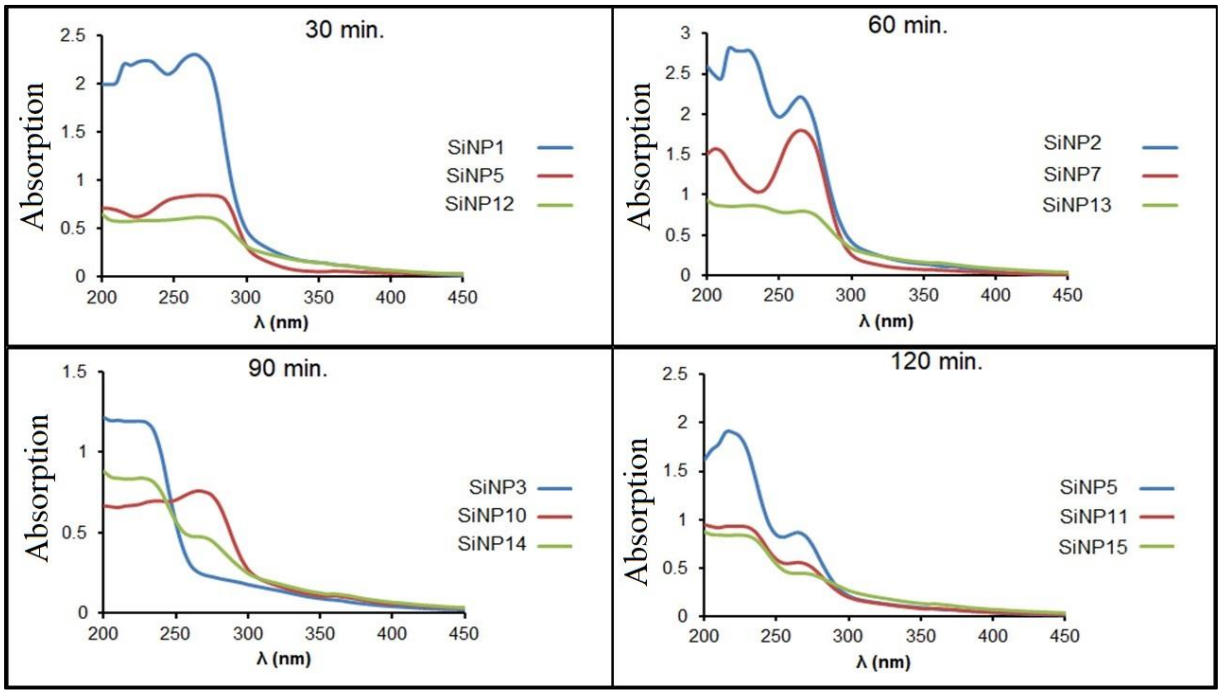

Figure 2. Reactions were conducted using 0.1 M ascorbic acid (1.25 mL) and 1.00 mL APTES at various durations to investigate the effect of temperature (40 °C, 50 °C, and 60 °C).

The broad bands could be attributed to n→π* or π→π* transitions, which usually occur in the near-UV and visible regions for ligands. The exact cause of fluorescence is not fully understood, but the emission can be attributed to two sources. One of these is related to an intrinsic band gap following core sp2 conjugation (sp2 clusters). The fluorescence from this source is controlled by the π states of sp2 regions. It is important to note that the σ and σ* states of sp2 clusters depend on the band gap between π and π* electronic levels. The radiative recombination of electron-hole pairs in these sp2 clusters is the cause of fluorescence.

NANOSAM
Journal of NanoScience in Advanced Materials

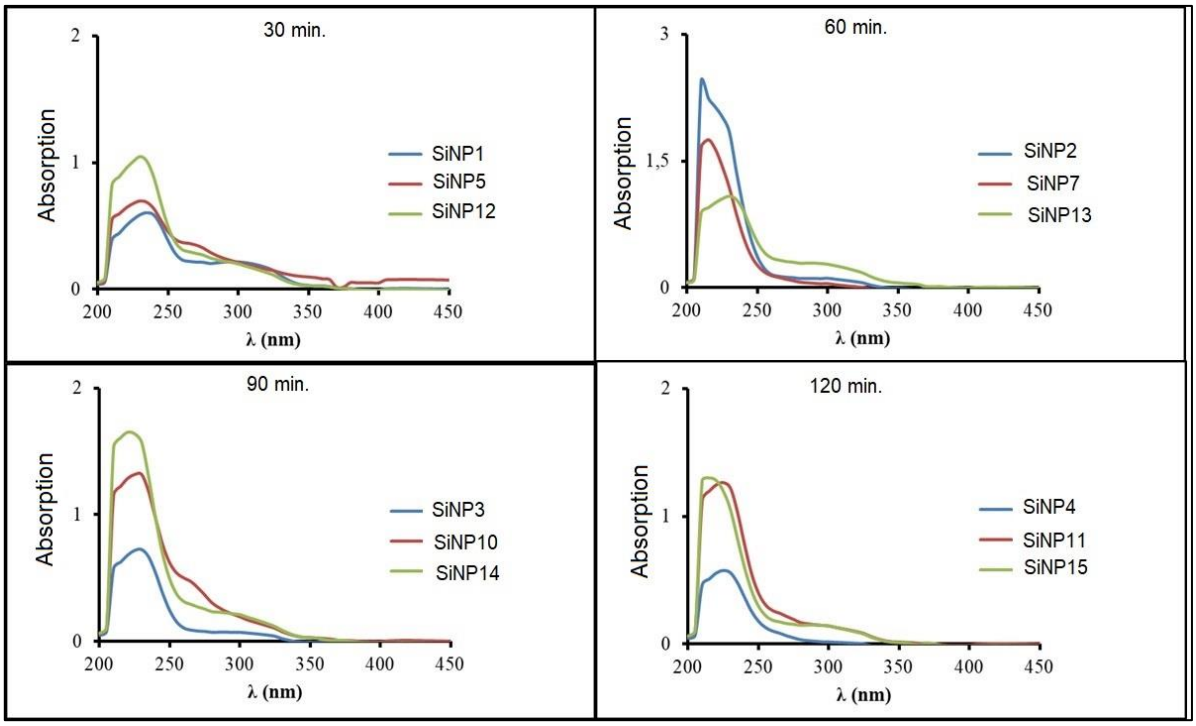

Figure 3. The effect of temperature (40 °C, 50 °C, and 60 °C) on reactions conducted with 0.1 M ascorbic acid (1.25 mL) and 1.00 mL APTES over various durations was evaluated, including changes observed approximately three months later.

APTES quantity: To examine the effect of APTES amount on the properties of the synthesized samples, a series of reactions were conducted while keeping the ascorbic acid amount (1.25 mL), reaction temperature (50 °C), and reaction time (60 minutes) constant. The APTES amounts used were 1.00 mL (SiNP7), 1.50 mL (SiNP16), 2.00 mL (SiNP17), 2.50 mL (SiNP18), and 3.00 mL (SiNP19). As shown in figure 7, SiNP7 exhibited earlier absorbance compared to the other samples in the graph, displaying absorbance in the 285-325 nm wavelength range and a wider band gap. As the amount of APTES increased, absorption occurred between 350-450 nm, with intensities ranked from strong to weak as follows: 1.50 mL, 3.00 mL, 2.00 mL, 2.50 mL, and 1.00 mL. Significant absorption characteristics of the nanoparticles were observed at 270 and 350 nm. The energy at 350 nm corresponds to the intrinsic direct Γ−Γ band gap of silicon, commonly seen as a peak in silicon nanoparticles, while the peak at 270 nm corresponds to the L−L transition of silicon. The presence of these two peaks indicates the existence existence of silicon particles in solution [15].

A strong absorption was observed with a peak centered around 348 nm [16]. As the amount of APTES increased, the quantity of silicon nanoparticles formed through reactions between APTES molecules also increased, resulting in two distinct absorbance maxima. Additionally, as shown in Figure 8, UV absorption analysis of the samples was repeated approximately three months later. As the samples aged, the absorption intensities in the 350-450 nm wavelength range decreased and shifted to the 200-325 nm range, as shown in Figure 8. In SiNP7, absorbance was observed only between 200-250 nm. The absorbances occurring beyond 250 nm indicate the presence of unreacted APTES molecules due to insufficient ascorbic acid.

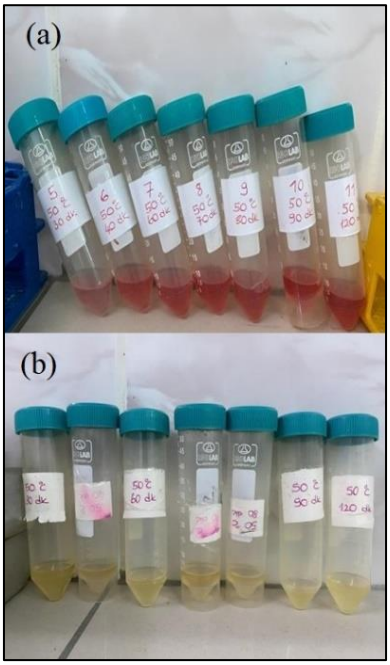

Figure 4. Color change of the synthesized samples when fresh (a) and after being stored for approximately 3 months (b).

NANOSAM
Journal of NanoScience in Advanced Materials

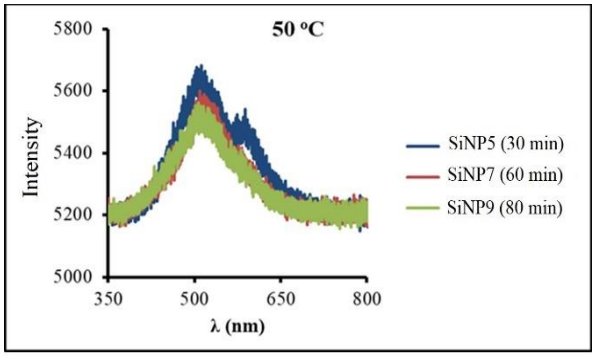

Figure 5. The effect of time (30 min, 60 min, and 80 min) on reactions carried out at 50 ºC using 0.1 M AA (1.25 mL) and 1.00 mL APTES.

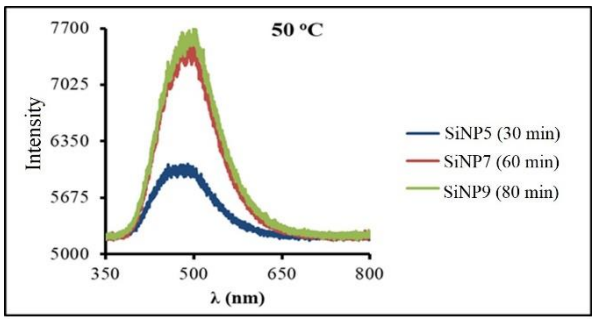

Figure 6. The change over approximately 3 months in reactions carried out at 50 ºC using 0.1 M AA (1.25 mL) and 1.00 mL APTES, observed at different times (30 min, 60 min, and 80 min).

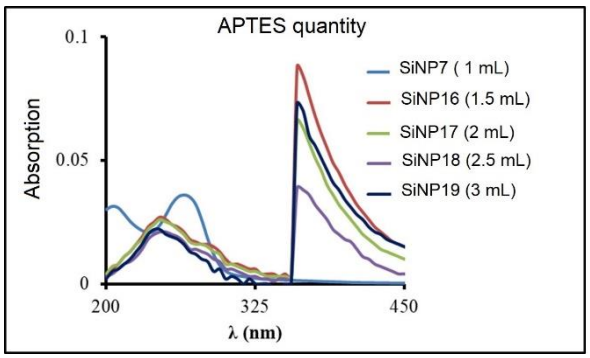

Figure 7. The effect of varying APTES amounts (1.00 mL, 1.50 mL, 2.00 mL, 2.50 mL, and 3.00 mL) was studied in reactions conducted at 50 °C for 60 minutes using 0.1 M ascorbic acid (1.25 mL).

To determine the optical band gap of the samples, a %R-wavelength graph was plotted and is illustrated in Figure 9. In this figure, nearly all samples exhibited a decline at the same wavelength, showing scattering behavior. SiNP16, SiNP18, and SiNP19 displayed a sharp emission around 250 nm, while SiNP17 exhibited a smaller emission at the same wavelength, and SiNP7 showed emission around 200 nm.

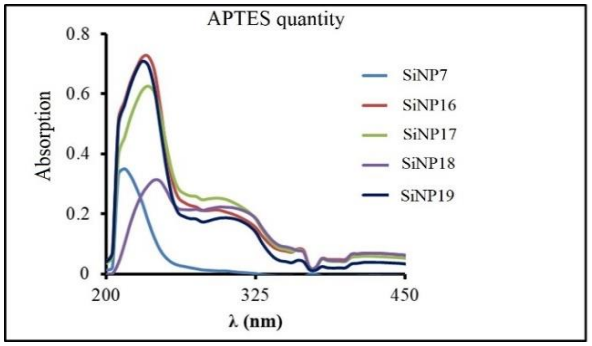

Figure 8. The changes in reactions conducted at 50 °C for 60 minutes using 0.1 M ascorbic acid (1.25 mL) were evaluated with varying APTES amounts (1.00 mL, 1.50 mL, 2.00 mL, 2.50 mL, and 3.00 mL) approximately three months later.

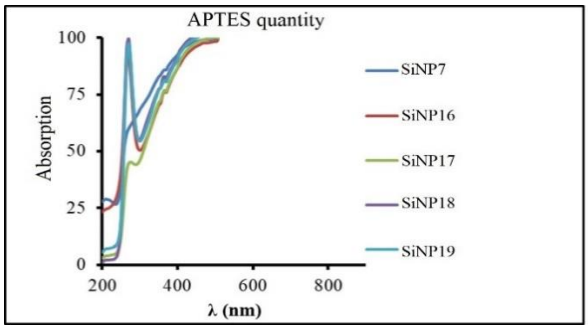

Figure 9. The effect of varying APTES amounts (1.00 mL, 1.50 mL, 2.00 mL, 2.50 mL, and 3.00 mL) on reactions conducted at 50 °C for 60 minutes using 0.1 M ascorbic acid (1.25 mL) was investigated.

Samples were excited using a 349 nm wavelength laser, and PL excitation and emission spectra were recorded at room temperature. The emission spectra obtained using photoluminescence spectroscopy are shown in Figure 10. As seen in figure 10, the emission intensity of all samples is nearly identical, and all samples exhibit emission intensity at approximately 520 nm wavelength. As seen in Figure 11, when the samples were stored at room temperature about three months, their emission intensities increased, and the broad band spectra, initially observed around 520 nm, shifted to 500 nm.

AA quantity: In order to observe the effect of ascorbic acid (AA) amount on the properties of samples synthesized at 50 °C for 60 minutes, the APTES amount was kept constant while varying the APTES amount was kept constant while varying the AA amount. In the first series of experiments, a set of syntheses was conducted at a reaction temperature of 50 °C and a reaction time of 60 minutes, using 1.50 mL of APTES and varying the amount of 0.1 M AA: 1.25 mL (SiNP16), 1.50 mL(SiNP20), 2.00 mL (SiNP21), and 2.50 mL (SiNP22).

NANOSAM
Journal of NanoScience in Advanced Materials

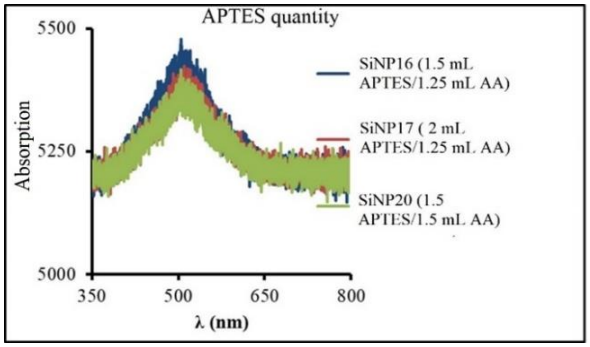

Figure 10. The effect of APTES amount (1.50 mL and 2.00 mL) in reactions conducted using 0.1 M AA (1.25 mL) at 50 °C for 60 minutes, and the effect of APTES amount (1.50 mL) in reactions conducted using 0.1 M AA (1.50 mL) under the same temperature and duration conditions.

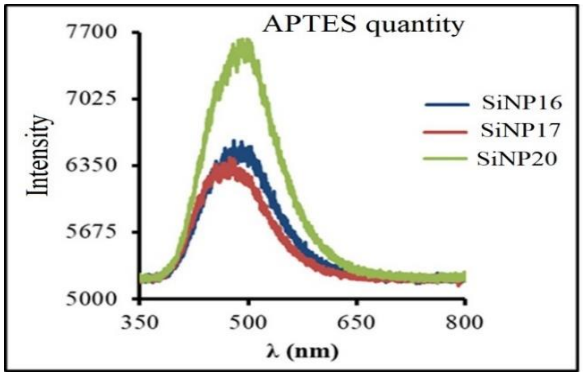

Figure 11. The change over approximately 3 months in reactions carried out at 50 ºC for 60 minutes using 0.1 M AA (1.25 mL) with varying amounts of APTES (1.50 mL and 2.00 mL), and in a reaction conducted under the same conditions with 0.1 M AA (1.50 mL) and 1.50 mL APTES.

As shown in Figure 12, the absorption intensity increased between 200-325 nm wavelengths as the AA amount increased. The addition of ascorbic acid as a reducing agent enhanced the formation of Si NPs. The synthesis with 1.25 mL of AA (SiNP16) exhibited significantly lower absorption intensity in the 200-325 nm wavelength range compared to the other samples, although previous syntheses conducted to determine the APTES amount showed more pronounced absorbance in this wavelength range. Therefore, it can be stated that the absorption intensities between 200-325 nm become more distinct as the AA amount increases. In the 325-450 nm wavelength range, only the synthesis with 1.25 mL of AA exhibited weak absorption intensity, while for other samples, the absorption intensity decreased as the AA amount increased.

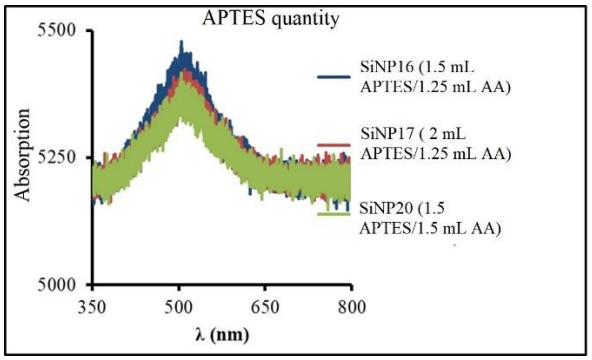

Figure 12. The effect of 0.1 M AA amount (1.25 mL, 1.50 mL, 2.00 mL, and 2.50 mL) in reactions conducted using 1.50 mL of APTES at 50 °C for 60 minutes.

TEM images: TEM analysis was performed to reveal the morphological structure, shape, and size characteristics of SiNPs. As shown in Figure 13, the SiNPs appeared as spherical particles with good monodispersity. It was clearly observed that nano particles were distributed in spherical shapes, with groups surrounding them. A total of 134 particles were measured using the ImageJ software at resolutions of 50 nm, 100 nm, 200 nm, and 500 nm. The data obtained from ImageJ were compiled in Excel, and the average particle size and standard deviation were calculated as 10.512±5.461 nm. This value is consistent with the results of similar studies in the literature [17].

As shown in Figure 14, the size of the nanoparticles increased as the amount of APTES increased, and it was observed that they were enclosed within surrounding groups. A total of 70 measurements were taken, and the average particle size and standard deviation were calculated as 11.884±7.205 nm.

In Figure 15, the TEM images of Si NPs show that they are enclosed within amine-silica chain groups. The average particle size and standard deviation were calculated as 8.508±2.832 nm based on 101 measurements. When the amounts of APTES and AA are similar, the particle size decreases.

NANOSAM
Journal of NanoScience in Advanced Materials

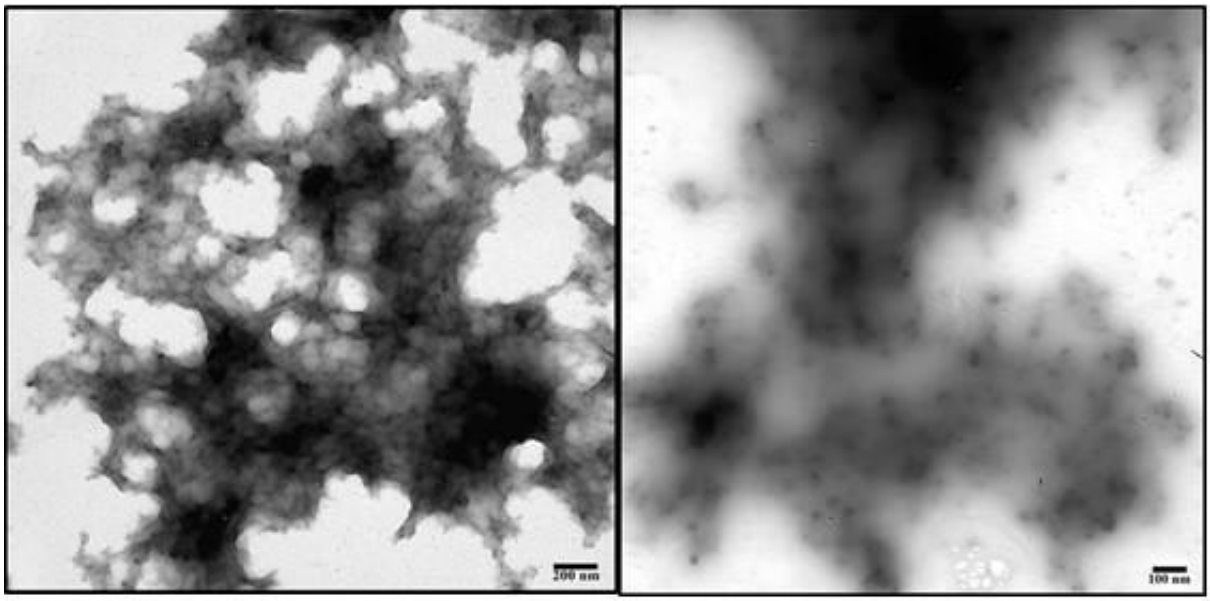

Figure 13. TEM images of Sample 7 (50 °C, 60 min, 1.00 mL APTES, 1.25 mL of 0.1 M AA).

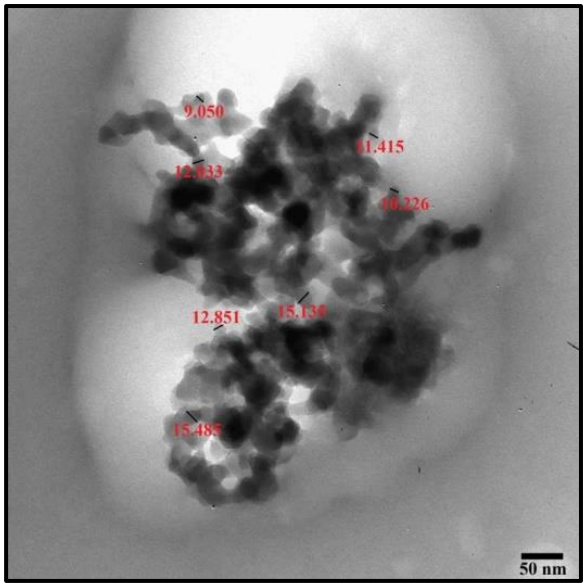

Figure 14. TEM image of Sample 16 (50 °C, 60 min, 1.50 mL APTES 0.1 M, 1.25 mL AA).

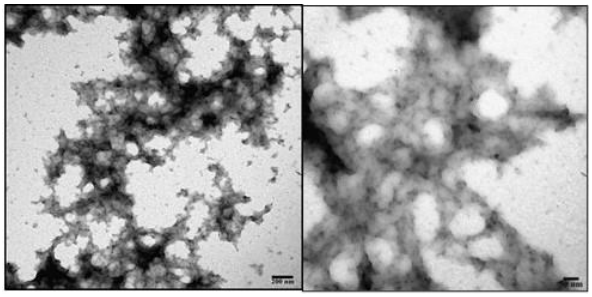

Figure 15. TEM images of Sample 20 (50 °C, 60 min, 1.50 mL APTES, 1.50 mL of 0.1 M AA).

3. Conclusion

In conclusion, this study systematically examined the influence of reaction parameters—including temperature, time, APTES, and ascorbic acid amounts—on the properties of silicon nanoparticles (Si NPs), focusing on particle size, UV absorption characteristics, photoluminescence [18], and stability over time. Key findings indicate that reaction temperature and duration notably affect the UV absorbance and particle formation, with higher temperatures enhancing UV absorbance due to the formation of more stable, smaller particles. The presence of a strong UV absorption band at 200–250 nm across all samples and the broadening of absorbance peaks at higher temperatures suggest an increase in nanoparticle synthesis rate and stability.

The photoluminescence (PL) analysis revealed that Si NPs exhibit a broad emission around 520 nm, which is consistent with the fluorescence properties reported in the literature for Si NPs. Notably, shorter reaction times resulted in narrower fluorescence spectra, indicating the impact of reaction duration on optical properties. Aging of the samples led to an increase in UV absorbance intensity, a shift towards shorter wavelengths, and heightened emission intensity, reflecting the stability and evolving interaction with UV light over time.

Variations in APTES and ascorbic acid quantities showed that higher APTES levels resulted in increased absorbance in the 350–450 nm range, with the formation of distinct absorbance peaks, suggesting more extensive silicon particle

formation. Conversely, increasing ascorbic acid as a reducing agent enhanced Si NP formation, particularly in the 200–325 nm wavelength range, with lower absorption intensities in this range when ascorbic acid levels were minimal. This emphasizes the role of ascorbic acid in influencing nanoparticle optical properties.

TEM images confirmed that Si NPs are spherical with good monodispersity, with particle sizes correlating with the APTES and ascorbic acid levels used. Higher APTES concentrations led to larger particles, while balanced amounts of APTES and ascorbic acid yielded smaller particles. The average particle size was in agreement with similar studies, highlighting that specific reaction conditions yield optimally sized and shaped Si NPs. This work sheds light on the influence of synthesis parameters on Si NPs, emphasizing their stability and dynamic optical characteristics.

Method

Materials APTES and ascorbic acid were used as analytical grade supplied from Sigma-Aldrich company. In this experimental procedure, a simple chemical synthesis method which cost less than 500 dollars was used at room temperature.

Synthesis of Silicon Nanoparticles (Si NPs) In this study, water-soluble Si NPs were synthesized using (3-aminopropyl)triethoxysilane (APTES,1-3 mL) as the silicon source and ascorbic acid (AA, 1.24-5 mL) as the reducing agent via a simple one-step method (figure 1) within 30-120 minutes. Once the reaction was completed, the reaction flask was removed from the water bath, cooled, and stored in Falcon tubes. No further purification was performed. Detailed information about the synthesis is provided in Table 1.

Figure 1. Reaction system of synthesis of Si/NP.

Characterization of Si NPs Ultraviolet-Visible Light (UV-Vis) Absorption Spectroscopy: Liquid samples were analyzed using a T80 UV/Vis Spectrometer (Model 1201, Shimadzu, Kyoto, Japan) with a quartz cuvette over the wavelength range of 200 nm to 900 nm. Both absorption and reflectance measurements were taken with this device.

Photoluminescence (PL) Spectroscopy: Luminescence measurements of the liquid samples were performed using a time-resolved low-photoluminescence system (Andor SR-5004-B1).

Transmission Electron Microscopy (TEM): Liquid samples were diluted 100-fold with distilled water and dropped onto copper grids. After allowing the grids to dry in an oven, TEM images were taken using a JEOL JEM-1400 PLUS transmission electron microscope.

Band Gap Calculations via Reflectance Measurements: The percentage reflectance (%R) versus wavelength graphs of the synthesized samples were obtained using the T80 UV/Vis spectrometer. McLean analysis was performed using these graphs. McLean analysis [12] for determining the transition type and calculating the optical band gap (Eg) has been completed. To determine the type of transition and calculate the optical band gap, McLean analysis is used as follows:

$$F(R).h\nu=k\,(h\nu - Eg)^{1/n} \quad \text{(Eq1)}$$

where k represents a constant related to the transition probability, and Eg is the optical band gap. F(R) is the Kubelka–Munk function:

$$F(R)=(1-R)^2/2R \quad \text{(Eq2)}$$

where R is the reflectance, and sss is the scattering factor.

Conflicts of Interest

The authors stated that did not have conflict of interests.

Author Contributions

GÇ: Corresponding author Ms. Çelik Gül, wrote the whole manuscript in English, including introduction and discussion section, rearranged the figures and tables, and has done the submission requirement.

ÇU: Performed experiments/data collection.

SB: Data analysis and interpretation, edited the paper, provided grammatical revisions to manuscript, provided revisions to scientific content of manuscript.

Data Availability Statement

The datasets generated during and/or analysed during the current study are available from the corresponding author on reasonable request.

References

[1] Anlar, H.G., Bacanlı, M., Başaran, N., Silikanın kullanım alanları ve silika maruziyetine bağlı olası toksik etkiler. Hacettepe University Journal of the Faculty of Pharmacy **39** (1), 17-29 (2019).

[2] Wu, S., et al., Biomimetic preparation and dual-color bioimaging of fluorescent silicon nanoparticles. Journal of the American Chemical Society **137** (46), 14726-14732 (2015).

[3] Pan, G-H., Barras, A., Boussekey, L., Addad, A., Boukherroub, R., Alkyl passivation and SiO2 encapsulation of silicon nanoparticles: preparation, surface modification and luminescence properties. Journal of Materials Chemistry C **1**, 5261-5271 (2013).

[4] Wen, Q., Jiang, C., Liu, W., Zeng, Z., Gao, J., Zheng, Y., Fluorescence determination of Ni2+ ions based on a novel nano-platform derived from silicon quantum dots. Silicon **14**, 385-392 (2020).

[5] Peng, F., Su, Y., Zhong, Y., Fan, C., Lee, S-T., He, Y., Silicon nanomaterials platform for bioimaging, biosensing, and cancer therapy. Accounts of Chemical Research **47** (2), 612-623 (2014).

[6] Zou, R., et al., Silica shell-assisted synthetic route for mono-disperse persistent nanophosphors with enhanced in vivo recharged near-infrared persistent luminescence. Nano Research **10** (6), 2070-2082 (2016).

[7] Li, X., et al., Europium functionalized ratiometric fluorescent transducer silicon nanoparticles based on FRET for the highly sensitive detection of tetracycline. Journal of Materials Chemistry C **5**, 2149-2152 (2017).

[8] Gürmen, S., Ebin, B., Nanopartiküller ve üretim yöntemleri-1. Metalurji Dergisi **150**, 31-38 (2008).

[9] Mallakpour, S., Naghdi, M., Polymer/SiO2 nanocomposites: production and applications. Progress in Materials Science **97**, 409-447 (2018).

[10] Ma, S., Chen, Y., Feng, J., Liu, J., Zuo, X., Chen, X., One-step synthesis of water-dispersible and biocompatible silicon nanoparticles for selective heparin sensing and cell imaging. Analytical Chemistry **88**, 10474-10481 (2016).

[11] Sypabekova, M., Hagemann, A., Rho, D., Kim, S., Review: 3-Aminopropyltriethoxysilane (APTES) deposition methods on oxide surfaces in solution and vapor phases for biosensing applications. Biosensors **13**, 36 (2022).

[12] McLean, T., *The absorption edge spectrum of semiconductors.* Progress in Semiconductors, Wiley (1960).

[13] Wamba, A.G.N., Lima, E.C., Ndi, S.K., Thue, P.S., Kayem, J.G., Rodembusch, F.S., et al., Synthesis of grafted natural pozzolan with 3-aminopropyltriethoxysilane: preparation, characterization, and application for removal of Brilliant Green 1 and Reactive Black 5 from aqueous solutions. Environmental Science and Pollution Research **24**, 21807-21820 (2017).

[14] Hughes, S., Dasary, S.S.R., Begum, S., Williams, N., Yu, H., Meisenheimer complex between 2,4,6-trinitrotoluene and 3-aminopropyltriethoxysilane and its use for a paper-based sensor. Sensing and Bio-Sensing Research **5**, 37-41 (2015).

[15] Bose, S., Ganayee, M.A., Mondal, B., Baidya, A., Chennu, S., Mohanty, J.S., et al., Synthesis of silicon nanoparticles from rice husk and their use as sustainable fluorophores for white light emission. ACS Sustainable Chemistry & Engineering **6**, 6203-6210 (2018).

[16] Zhang, H-J., Xiong, H-M., Ren, Q-G., Xia, Y-Y., Kong, J-L., ZnO@silica core–shell nanoparticles with remarkable luminescence and stability in cell imaging. Journal of Materials Chemistry **22**, 13159-13165 (2012).

[17] Zarschler, K., et al., Ultrasmall inorganic nanoparticles: State-of-the-art and perspectives for biomedical applications. Nanomedicine **12** (6), 1663-1701 (2016).

[18] Sündü, B., Türkkan, A., Eroglu Z., Metin O., In situSynthesis of 2D Bismuth/Graphitic Carbon Nitride Heterojunctions for the Visible Light-Driven Organic Dye Degradation. Journal of NanoScience in Advenced Materials, **2** (2)**,** 36-44 (2023)